

BVRI Photometry of Supernovae

Wynn C. G. Ho^{1,2}, Schuyler D. Van Dyk³, Chien Y. Peng⁴, Alexei V. Filippenko⁵, Douglas C. Leonard⁶,
Thomas Matheson⁷, Richard R. Treffers⁸

Department of Astronomy, 601 Campbell Hall, University of California, Berkeley, CA 94720-3411

and

Michael W. Richmond⁹

Department of Physics, Rochester Institute of Technology, Rochester, NY 14623-5603

ABSTRACT

We present optical photometry of one Type II_n supernova (1994Y) and nine Type Ia supernovae (1993Y, 1993Z, 1993ae, 1994B, 1994C, 1994M, 1994Q, 1994ae, and 1995D). SN 1993Y and SN 1993Z appear to be normal SN Ia events with similar rates of decline, but we do not have data near maximum brightness. The colors of SN 1994C suggest that it suffers from significant reddening or is intrinsically red. The light curves of SN 1994Y are complicated; they show a slow rise and gradual decline near maximum brightness in *VRI* and numerous changes in the decline rates at later times. SN 1994Y also demonstrates color evolution similar to that of the SN II_n 1988Z, but it is slightly more luminous and declines more rapidly than SN 1988Z. The behavior of SN 1994Y indicates a small ejecta mass and a gradual strengthening of the H α emission relative to the continuum.

Subject headings: supernovae: general – supernovae: individual (1993Y, 1993Z, 1993ae, 1994B, 1994C, 1994M, 1994Q, 1994Y, 1994ae, 1995D)

¹Also associated with Space Sciences Laboratory, and Department of Physics, University of California, Berkeley.

²Current address: Department of Astronomy, Cornell University, Ithaca, NY 14853; e-mail wynrho@astro.cornell.edu.

³Current address: IPAC, 100-22 Caltech, Pasadena, CA 91125; e-mail vandyk@ipac.caltech.edu.

⁴Current address: Steward Observatory, University of Arizona, Tucson, AZ 85721; e-mail cyp@as.arizona.edu.

⁵E-mail alex@astro.berkeley.edu.

⁶Current address: Department of Astronomy, University of Massachusetts, Amherst, MA 01003-9305; e-mail leonard@nova.astro.umass.edu.

⁷Current address: Harvard-Smithsonian Center for Astrophysics, 60 Garden St., Cambridge, MA 02138; e-mail tmatheso@cfa.harvard.edu.

⁸E-mail treffers@pacbell.net.

⁹E-mail mwrsp@rit.edu.

1. Introduction

Supernova (SN) light curves reveal the structure of the stellar progenitors and reflect the underlying energy sources created in the explosion. They have also been the primary tool for intercomparison of individual events and selection of subsamples of supernovae (SNe) for use as distance indicators. Direct comparisons of peak luminosities and multiband light curves with the predictions of theoretical models lead to a better understanding of supernova explosions. Useful reviews of the optical light curves of SNe are given by Doggett & Branch (1985), Kirshner (1990), Wheeler & Harkness (1990), Patat et al. (1994), Leibundgut (1996), and Suntzeff (1996), among others.

We have been engaged in systematic optical monitoring of bright, relatively nearby SNe. These include hydrogen-rich objects (Type II), as well as the various kinds of hydrogen-deficient SNe (Types Ia, Ib, and Ic). (For a summary of the spectroscopic properties of SNe, see Filippenko 1997.) Here we report our results for nine SNe Ia and one peculiar SN II, from data obtained in 1993–1995. Section 2 discusses the discoveries of the SNe, and Section 3 contains a description of the observations. The “template subtraction” method of photometry used to extract the light of SNe from their environs is presented in Section 4. Section 5 describes the calibration of the measurements onto the standard Johnson-Kron-Cousins system. The SN light curves and color curves appear in Sections 6 and 7, respectively, while estimates of the absolute magnitudes are in Section 8. Section 9 summarizes our results. UT dates are used in all cases.

2. Discoveries

The discoveries of the supernovae presented here were made by several groups. SN 1993Y (Fig. 1) in UGC 2771 was discovered on 1993 September 18, about $9''$ east and $39''.6$ north of the galaxy’s nucleus, with the 1.2-m Oschin telescope as part of the second Palomar Sky Survey (Mueller 1993). Accurate position measurements of the object resulted in $\alpha_{1950} = 3^h 28^m 6^s.75$, $\delta_{1950} = +39^\circ 34' 51''.9$ (Balam 1993). A spectrum taken on September 22 showed SN 1993Y to be of Type Ia about three weeks past maximum brightness (Dressler & Sargent 1993). Another spectrum taken on September 25 showed that it was close to one month past maximum (Filippenko & Matheson 1993).

SN 1993Z (Fig. 2) in the Sab galaxy NGC 2775 was found on 1993 September 23, about $15''$ west and $42''$ south of the nucleus, as part of the Leuschner Observatory Supernova Search (LOSS) using a 0.76-m telescope (Treffers et al. 1993). The accurate position measurement of the SN is $\alpha_{1950} = 9^h 7^m 40^s.18$, $\delta_{1950} = +7^\circ 13' 56''.1$ (Balam 1993). A spectrum taken on September 25 indicated SN 1993Z to be of Type Ia about four weeks past maximum (Treffers et al. 1993).

SN 1993ae (Fig. 3) in UGC 1071 was found with the 0.9-m Schmidt telescope at the Observatoire de la Cote d’Azur (OCA) on 1993 November 7.92; the SN was located at $\alpha_{1950} = 1^h 27^m 16^s.08$, $\delta_{1950} = -2^\circ 14' 5''.5$ (Pollas 1993). Spectroscopy on November 11.2 showed that SN 1993ae was a normal Type Ia about 10 d after maximum with an expansion velocity of about 10000 km s^{-1} from Si II $\lambda 6355$ (Cappellaro & Bragaglia 1993). The supernova was located about $16''$ east and $24''$ north of the nucleus.

SN 1994B (Fig. 4) was discovered on 1994 January 16.98 in an anonymous galaxy, again using the OCA 0.9-m Schmidt telescope; the supernova position was at $\alpha_{1950} = 8^h 17^m 51^s.64$, $\delta_{1950} = 15^\circ 53' 20''.5$, or $4''.2$ east and $3''.9$ north of the center of the host face-on spiral galaxy (Pollas 1994). A spectrum obtained on January 19 suggested that SN 1994B was of Type Ia near maximum; the broad Si II $\lambda 6355$ absorption trough was visible, and a redshift $z = 0.089$ of the parent galaxy was also determined from the H II region

on which SN 1994B was superposed (Filippenko & Matheson 1994).

SN 1994C (Fig. 5) was discovered on 1994 March 5 at $\alpha_{1950} = 7^h53^m8^s.7$, $\delta_{1950} = 45^\circ0'20''.8$ during the second Palomar Sky Survey (Mueller & Mendenhall 1994). It was confirmed as a SN on March 9 (Djorgovski, Thompson, & Smith 1994). SN 1994C was classified on March 12 as a Type Ia about 20 d past maximum, and the host galaxy’s redshift was determined to be $z = 0.051$ (Riess, Challis, & Kirshner 1994). It was located about $3''$ west and $6''$ north of the anonymous galaxy’s nucleus.

SN 1994M (Fig. 6) in NGC 4493 was found by Wild (1994) at Zimmerwald, University of Berne, on 1994 April 29.9; the SN position was $\alpha_{1950} = 12^h28^m35^s.1$, $\delta_{1950} = 0^\circ52'54''$, about $3''$ west and $28''$ south of the nucleus. A spectrum taken on May 4.14 showed it to be of Type Ia very close to maximum light (Schmidt, Kirshner, & Peters 1994).

SN 1994Q (Fig. 7) was found with the OCA 0.9-m Schmidt telescope on 1994 June 2.92 at $\alpha_{1950} = 16^h48^m11^s.64$, $\delta_{1950} = +40^\circ31'1''.1$, or $0''.4$ west and $3''.5$ south of an anonymous galaxy’s nucleus (Pollas & Albanese 1994). A spectrum taken on June 3 suggested that SN 1994Q was of Type Ia about one week past maximum (Filippenko, Matheson, & Barth 1994).

SN 1994ae (Fig. 8) in the Sc galaxy NGC 3370 was discovered on 1994 November 14 by LOSS (Van Dyk et al. 1994) long before maximum light; various estimates of the date of maximum visual brightness were November 30 (Nakano et al. 1994), December 1 (Patat, Vician, & Szentasko 1994), and prior to December 6 (Vanmunster, Villi, & Cortini 1994). The accurate position is $\alpha_{1950} = 10^h44^m21^s.52$, $\delta_{1950} = +17^\circ32'20''.7$ (Nakano, Kushida, & Kushida 1994), which is $30''.3$ west and $6''.1$ north of the galaxy nucleus. A spectrum taken on November 23.16 indicated SN 1994ae to be of Type Ia; the measured expansion velocity for the Si II $\lambda 6355$ line was 11000 km s^{-1} (Iijima, Cappellaro, & Turatto 1994).

SN 1995D (Fig 9) in the S0 galaxy NGC 2962 was found apparently on the rise on 1995 February 10.76, using a 0.25-m telescope at the Yatsugatake South Base Observatory (Kushida, Nakano, & Kushida 1995) at $\alpha_{2000} = 9^h40^m54^s.79$, $\delta_{2000} = +5^\circ8'26''.6$, about $11''$ east and $90''.5$ south of the galactic nucleus. A spectrum obtained on February 13.18 confirmed it as a Type Ia, about one week before maximum; the spectrum was dominated by P-Cygni lines of intermediate-mass elements on a very blue continuum, and the deduced expansion velocity for Si II $\lambda 6355$ was 10900 km s^{-1} (Benetti, Mendes de Oliveira, & Manchado 1995).

SN 1994Y (Fig. 10) in the Sbc galaxy NGC 5371 was discovered on 1994 August 19.15 with a 0.9-m telescope at McDonald Observatory (Wren 1994). Images obtained as part of the LOSS showed it to be about $34''$ west and $11''$ north of the nucleus, on the rise from August 12 to August 16, and not visible on August 3, 6, and 9 (Paik et al. 1994). A spectrum taken on August 25 identified it as a Type II (Jiang, Liu, & Hu 1994). Furthermore, Clocchiatti et al. (1994) took a spectrum on August 27.15, which showed the Balmer emission lines without the characteristic P-Cygni profiles; rather, there were narrow lines on top of broad bases, thereby resulting in the classification of SN 1994Y as a Type IIn (see Filippenko 1997). Also evident in a spectrum taken on 1995 February 8 was a narrow absorption feature at 6622 \AA superimposed on the strong H α line, signifying a large amount of circumstellar material (Wang et al. 1995). Accurate position measurements yielded $\alpha_{1950} = 13^h53^m30^s.57$, $\delta_{1950} = +40^\circ42'32''.8$ (Boattini & Tombelli 1994).

3. Observations

Observations were made at Lick Observatory with the Nickel 1-m reflector and standard Johnson-Kron-Cousins *BVRI* filters. The telescope utilizes a Loral 2048×2048 pixel CCD ($15 \mu\text{m pixel}^{-1}$), which we

binned 2×2 to yield a plate scale of $0''.37 \text{ pixel}^{-1}$. The full-width at half-maximum (FWHM) of stellar objects generally varied from about $1''.5$ to $2''$. The CCD images were bias corrected using an average of several bias images. They were also flattened by the average of several flatfield images of the twilight sky. Exposure times were as short as 120 s for SN 1994ae near maximum light to 1800 s for deeper late-time and template images. However, some images were combined to give a longer overall exposure time. Figures 1–10 illustrate Lick images of the ten SNe, their host galaxies, and the stars in the field that were used as comparisons (henceforth referred to as field stars).

SN 1993Y, SN 1993Z, and SN 1994Y were also observed at Leuschner Observatory as part of the Berkeley Automatic Imaging Telescope (BAIT) project, which employed 50-cm and 76-cm telescopes (see Filippenko 1992; Richmond, Treffers, & Filippenko 1993; Richmond et al. 1996; and references therein). Each telescope was equipped with a 512×512 pixel CCD with a plate scale of about $0''.65 \text{ pixel}^{-1}$, and stellar objects generally had a FWHM of about $3''$ to $4''$. The filters were made according to the characteristics described by Bessell (1990). The images were bias corrected with the median of five bias images taken each afternoon. Five flat-field images of the twilight sky were used to determine a median image, which was then used to flatten the data. Exposure times were between 120 and 900 s. SN 1993Y was observed from 1993 September 26 through December 20, SN 1993Z from 1993 September 23 through 1994 February 1, and SN 1994Y from 1994 August 22 through December 7.

In addition, three images of SN 1994Y were taken at Kitt Peak National Observatory on 1995 January 28, using a 0.9-m telescope and Tektronix 2048×2048 pixel CCD ($24 \mu\text{m} \text{ pixel}^{-1}$). They were each 300-s exposures at a plate scale of $0''.68 \text{ pixel}^{-1}$ and FWHM from $2''$ to $3''$.

4. Photometry

To determine the instrumental magnitudes of most of these various SNe, we use the technique of template subtraction described in Richmond et al. (1995; see also Filippenko et al. 1986) to minimize the light contamination by the background galaxy. This involves taking a “template” image of the galaxy long after the supernova has faded. The template image was matched to each early-time image by registering the template using several field stars in common. The template was obtained under superior seeing conditions and was then convolved with a Gaussian to match the widths of the point-spread function (PSF) of each early-time image. The magnitudes of the field stars for both the template and early-time images were measured using a circular aperture of 15 pixels radius and a sky annulus of width 10 pixels. Comparing the magnitudes, an average scale factor was obtained and used to subtract the template image from the early-time image. The flux scale factor varied by $\leq 10\%$ typically from star to star within a given frame. The resulting template-subtracted image showed only the SN and, occasionally, the small residuals of the field stars and the host galaxy nucleus. The SN magnitude was then measured with negligible contamination from the galaxy light.

For SNe 1993ae, 1994M, and 1995D, template subtraction was not needed, because the SN was sufficiently far from the galactic nucleus and in a region of relatively uniform background. Simple aperture photometry was performed in these cases, with a circular aperture of 10 or 15 pixels radius and a 10-pixel-width sky annulus.

PSF-fitting photometry, via IRAF¹⁰/DAOPHOT (Stetson 1987), was performed for SN 1994Y and for

¹⁰IRAF (Image Reduction and Analysis Facility) is distributed by the National Optical Astronomy Observatories, which are

the Leuschner observations of SN 1993Y. In both cases, the model PSF was constructed using bright, isolated field stars on each of the images. SN 1993Y was far enough from the host galaxy nucleus that the background was negligible in all bands.

5. Calibrations

On particular nights when the conditions were photometric, standard star fields from Landolt (1992) were observed in *BVRI*, along with images of the SN. The instrumental magnitudes of these stars were determined using either a 10- or 15-pixel-radius circular aperture and a 10-pixel-width sky annulus. Using IRAF, the photometric instrumental magnitudes were converted to apparent magnitudes with the transformation equations

$$b = (B - V) + V + b_1 + b_2 X_b + b_3 (B - V) \quad (1)$$

$$v = V + v_1 + v_2 X_v + v_3 (B - V) \quad (2)$$

$$r = V - (V - R) + r_1 + r_2 X_r + r_3 (V - R) \quad (3)$$

$$i = V - (V - R) - (R - I) + i_1 + i_2 X_i + i_3 (R - I), \quad (4)$$

where *bvri* are instrumental magnitudes, *BVRI* are standard apparent magnitudes, and *X* are the airmass values. The second-order extinction terms were set to zero. The results, along with the number of Landolt fields observed and used on each night to determine the photometric solution, are shown in Table 1. In solving these equations, the standard deviations in the residuals were on the order of a few hundredths of a magnitude. Thus, the net uncertainty of the fit can be taken to be ≤ 0.03 mag.

In each of Figures 1–10, the labeled field stars were the comparisons used to determine the apparent magnitude of the respective SN. Each field star’s instrumental magnitude was measured, again using the same aperture and sky annulus as above, and transformed with Equations (1)–(4) into apparent magnitudes. Table 2 lists the results and their respective uncertainties. The images were fairly clean, so that cosmic ray hits near the stars of interest occurred only rarely. In such cases where the cosmic-ray pixels could be easily identified, they were smoothed by linear interpolation using nearby pixels. In cases when there were no photometric observations made, the apparent magnitudes of the field stars were obtained from Riess (1996). Also, observations of SNe 1993Z, 1994ae, 1995D, and 1994Y occurred on multiple nights under photometric conditions; the night with the smallest photometric uncertainties was adopted as the standard. Comparisons of our field star calibrations with Riess (1996) and Riess et al. (1999) were made, whenever possible, and the results were generally quite consistent.

Each SN instrumental magnitude was then converted into an apparent magnitude on the standard Johnson-Kron-Cousins *BVRI* system using a weighted mean of the difference between the instrumental and apparent magnitudes of the field stars. Tables 3–6 present these magnitudes along with their uncertainties. In addition, a comparison of the SN 1994Y data using PSF fitting versus template-subtraction yielded negligible differences when the SN was bright. Comparisons with the results of Riess (1996) and Riess et al. (1999) generally show good agreement for the objects and epochs in common: the mean difference for 34 points is ~ 0.01 mag, and the dispersion is ~ 0.07 mag. However, there may be a slight systematic trend,

namely our average values are ~ 0.04 , 0.02 , 0.01 mag brighter in B , V , and R , respectively, and ~ 0.03 mag fainter in I than those of Riess (1996) and Riess et al. (1999).

Finally, we note that the transformation equations (1)-(4), which were used on photometric nights at Lick to derive apparent magnitudes of the field stars from their instrumental magnitudes, are implicitly assumed to be valid for the Leuschner and KPNO data. From the apparent magnitudes of the field stars, we find the scaling relation for the nights that were not photometric and scale the SN instrumental magnitude to an apparent magnitude. Although the Loral chips were changed in the middle of the Lick program, the two CCDs were very similar (both Loral) and the filters remained the same, so nearly the same transformation should apply. The lack of independent transformations for the Leuschner and KPNO data increases the uncertainties of these data but by an amount that is difficult to quantify. Unfortunately, the Leuschner system that was used is no longer available for calibration; however, we still obtain consistent results between Lick and Leuschner. There were only three KPNO measurements, and again, they are consistent with the other results.

6. Optical Light Curves

6.1. Type Ia Supernovae

Figure 11 shows the light curves of SN 1993Y, and Figure 12 shows the light curves of SN 1993Z. The light curves of SNe 1993ae, 1994B, 1994C, 1994M, 1994Q, 1994ae, and 1995D are shown in Figure 13. The line segments connecting the points have no significance other than to aid the reader in distinguishing between different SNe and to indicate general trends.

The time of maximum light for SN 1993Y is uncertain. Based on its spectra, it was estimated to be either around August 26 (Filippenko & Matheson 1993) or September 1 (Dressler & Sargent 1993). For this paper, we adopt August 26 as the date of peak brightness. The observations of SN 1993Y are therefore from 31 d to 137 d past maximum. Normal Type Ia SNe show a decrease in the decline rate to a slow linear magnitude decline at around 40 d past maximum in V and R and at ~ 60 d in I . This is evident in our light curves for SN 1993Y, with the change in slope occurring some time between October 1 (~ 36 d after maximum) and October 18 (~ 53 d after maximum) in V and R , and around October 27 (~ 62 d after maximum) in I . The data after the onset of slow decline was fit to a line using a weighted least-squares fit algorithm (Press et al. 1992). The corresponding rates of slow decline for SN 1993Y are shown in Table 7, along with a comparison to the rates of slow decline for two normal SNe Ia, SN 1980N (decline rates starting from 42 d past maximum; Hamuy et al. 1991) and SN 1989B (decline rates from 42 d to 131 d past maximum; Wells et al. 1994). As is evident, the results for SN 1993Y are in agreement with both SNe 1980N and 1989B.

We adopt August 28 as the date SN 1993Z reached maximum brightness; thus, the observations presented here are from 26 d to 258 d past maximum. By fitting to different segments of our data in R , we determine that a change in the rate of decline occurred between September 26 (~ 29 d after maximum) and October 22 (~ 55 d after maximum), which is the case for normal Type Ia SNe. Using the same method described above and fitting only to the data after the onset of the slow linear magnitude decline, the rates for SN 1993Z are shown in Table 7. As in the case of SN 1993Y, the rates of slow decline for SN 1993Z are in agreement with the respective values of the two normal SNe Ia, SNe 1980N and 1989B.

The dates of maximum B -band brightness of SNe 1993ae, 1994M, 1994Q, and 1994ae were determined from their light curves to be 1993 November 2.1, 1994 May 3.6, 1994 May 28.9, and 1994 November 29,

respectively (Riess 1996); hence, our first observation of SN 1994ae is just 2 d after B maximum. Those of SNe 1994B and 1994C were determined from their spectra to be 1994 January 27 and 1994 February 28, respectively (Riess et al. 1999).

Sadakane et al. (1996) present extensive light curves in VRI during the first 100 d for SN 1995D, as well as several spectra near maximum brightness. They determine V maximum to be on February 21.5. It is also seen from their light curves that I maximum occurs prior to the date of V maximum. Comparison of our data with their photometry at about the same epoch shows very good agreement. At the first epoch in common, our data in V are fainter by 0.01 mag, which is well within the uncertainties. Sadakane et al. do not have R and I data at this epoch. However, they have data 2 d prior and 3 d after this common epoch, and our R and I data do lie between these points. At the second epoch in common, our V and R data are brighter by ≤ 0.07 mag, and our I data is fainter by 0.21 mag, all within a few times the uncertainties. Riess (1996) gives the date of B maximum to be February 21.3.

6.2. Type II_n Supernova 1994Y

Early-time spectra of SN 1994Y reveal Balmer emission lines on a wide base, while at later times the Balmer lines broaden; at all times there is an absence of narrow absorption lines seen in some other Type II_n supernovae (Filippenko 1997). Figure 14 shows the light curves for SN 1994Y. From the paucity of data in B , it is difficult to say how long SN 1994Y stayed near maximum, but it is apparent that SN 1994Y had a “plateau”-like phase near maximum with a duration of about 30 d in V , 40 d in R , and 20 d in I . This plateau’s appearance, however, differs from that seen in conventional SNe II-P (Doggett & Branch 1985).

An estimate of the times and magnitudes of peak brightness was made by eye using the data between JD 2,449,580 and 2,449,700; Table 8 lists the results. The uncertainty was estimated from the breadth of the maximum and the abundance of data points near the peak. In B , the light curve seems to indicate a rapid rise and fall. In V and R , it reaches the “plateau” around (or slightly before) JD 2,449,600 and only gradually rises and falls. In particular, there is no clear indication of the time of V maximum, which may have occurred in the gap between our observations. R maximum seems to have occurred late in the plateau. In I , there is a more distinct peak.

It is evident from the R and I light curves that there is a change in the post-maximum rate of decline around JD 2,449,800 — the decline rates become steeper. There is a similar change in V at about JD 2,449,860. We fit a linear decline to the data in V after JD 2,449,700 but prior to 2,449,860, and in R for all data after JD 2,449,800. The calculated rates of decline are shown in Table 7, along with the decline rates for another Type II_n, SN 1988Z (rate from 110 d to 450 d past maximum; Turatto et al. 1993), and a peculiar Type II, SN 1993J (rate from about 200 d to 400 d after maximum; Richmond et al. 1996). SN 1994Y demonstrates a much more rapid decline than SN 1988Z, but one that is on the same order of magnitude as SN 1993J.

Two indications imply that the mass of the ejecta in SN 1994Y was small. The brightness of SN 1994Y remained at a plateau for only several weeks (instead of several months, as do most SNe II-P), which suggests a small ejecta mass, since the duration of the plateau phase depends on how long the effective photosphere takes to work its way back through the hydrogen envelope of the star into the inner regions. A short phase indicates that the hydrogen envelope is not massive (or that the SN was expanding much more quickly than usual). Also, Barbon et al. (1995) and Richmond et al. (1996) indicate in the case of SN 1993J that the small amount of mass ejected, implied from its double peak, leads to a decrease in the efficiency of γ -ray trapping;

this generates a faster rate of decline than the 0.98 mag per 100 d resulting from the radioactive decay of ^{56}Co , which powers the late-time light curves of normal Type II-P SNe. The similarity in the decline rates of SN 1994Y and SN 1993J, again, suggests that the ejecta of SN 1994Y were also small in mass.

Finally, the B and V light curves exhibit another change in their rates of decline beginning around JD 2,449,925, leveling off to about 0.14–0.15 mag per 100 d. This is similar to the very late-time decline rate of 0.15–0.16 mag per 100 d seen in SN 1988Z between 730 d and 1150 d (Turatto et al. 1993), which is a period well after our observations of SN 1994Y. We suspect that interaction of the ejecta with circumstellar gas is providing additional light, as in the case for SN 1988Z. However, the flattening of the light curves suggests that this process becomes more pronounced at an earlier time in SN 1994Y, which again may be a result of the small ejecta mass.

7. Optical Color Curves

Figure 15 shows the color curves of the nine Type Ia SNe. Note that these values have not been corrected for reddening. There are large variations in the late-time $R - I$ template color curve given by Riess, Press, & Kirshner (1996); we have chosen a typical one, but there is a substantial difference between our observations and this template. SN 1993Y may be more reddened than most of the other SNe Ia presented here. The proximity of SN 1994C to the host galaxy’s nucleus and the SN’s very red color at early times suggest that it suffered significant reddening or was intrinsically red. Comparisons of our colors for SN 1995D with the color curves from Sadakane et al. (1996) show good agreement.

Figure 16 presents the color curves of SN 1994Y. SN 1988Z had an initial $B - V \approx 0.4$ mag, followed by a leveling off at later times to $B - V \approx 0.64$ mag (Turatto et al. 1993). Due to the ambiguity of the time of maximum for SN 1994Y, it is difficult to indicate the colors at peak brightness. However, at the assumed time of B maximum, $B - V$ is between 0.12 and 0.25 mag. Furthermore, $B - V$ at later times also seems to be approaching a plateau around 0.5 mag. $V - R$ appears to increase monotonically, almost linearly, with time. $R - I$, on the other hand, is -0.15 mag about two weeks prior to B maximum, reddens to a peak at or above 0.27 mag some time after two months, then turns blueward for the duration of our observations, ending a year from B maximum at -0.78 mag. The $V - R$ and $R - I$ color curves at late times show the growing strength of R relative to V and I , thus suggesting that the $\text{H}\alpha$ line is getting stronger relative to the continuum, and optical spectra confirm this conclusion (Filippenko 1997; Matheson & Filippenko 1999, private communication).¹¹ This explains the lack of a change in the rate of decline at late times of the R light curve, since most of the light is concentrated in the $\text{H}\alpha$ emission.

8. Absolute Magnitudes

We can calculate the absolute magnitude of SN 1994Y, for which we have data near maximum light. Burstein & Heiles (1984) determine the Galactic extinction to NGC 5371 (the host of SN 1994Y) to be $A_B = 0.00$ mag. Using the distance modulus to NGC 5371, $\mu = 32.89$ mag (Tully 1988), the resulting absolute magnitudes are shown in Table 8. Peak B brightness is $M_{B,max} = -18.37$ mag. Average Type II supernovae have $M_{B,max} = -16.89$ mag, but the dispersion is quite large, $\sigma = 1.35$ mag (Miller & Branch 1990). Like

¹¹The $\text{H}\alpha$ equivalent width is 1200 Å on 1995 January 25, ~ 2100 Å on April 22, and even larger at later times.

SN 1988Z, which has a $M_{B,max} \leq -18.0$ mag (Turatto et al. 1993), SN 1994Y is more luminous than the typical SN II but not abnormally so.

9. Conclusions

We presented *BVRI* photometry of the Type IIn SN 1994Y and the Type Ia SNe 1993Y, 1993Z, 1993ae, 1994B, 1994C, 1994M, 1994Q, 1994ae, and 1995D. All observations were done using telescopes of diameter 1 m or less. Light curves of SN 1993Y and SN 1993Z exhibit late-time rates of decline very similar to those of typical SNe Ia. The color curves of SN 1993Y suggest that it suffers more reddening than most of the other SNe Ia presented here. SN 1994C may also have been significantly reddened or was intrinsically red. The light curves of SN 1994Y show that it remained at a plateau near maximum light for several weeks, with no definitive date of peak brightness. The light curves also suggest that the ejecta mass was small. The estimated absolute magnitude of SN 1994Y shows that it, like the SN IIn 1988Z, was slightly more luminous than normal SNe II.

We are grateful to A. J. Barth, B. Leibundgut, and D. Schlegel for their assistance in obtaining some of the data. We would also like to express our appreciation to A. G. Riess for determining the ages of some of the SNe Ia and for providing helpful comments. The thoughtful and extensive suggestions of the anonymous referee led to substantial improvements in this paper. The research of A.V.F.'s group was supported by NSF grants AST-8957063, AST-9115174, AST-9417213, and AST-9987438, as well as by NASA through grants GO-6043 and GO-6584 from the Space Telescope Science Institute (which is operated by AURA, Inc., under NASA contract NAS 5-26555). A.V.F. also thanks the Guggenheim Foundation for a Fellowship. We are grateful to Sun Microsystems, Inc. (Academic Equipment Grant Program) and Photometrics, Ltd. for equipment donations to the telescopes (BAIT) at Leuschner Observatory. The supernova search and follow-up efforts with BAIT were the precursors to (and testbeds of) the Lick Observatory Supernova Search with the Katzman Automatic Imaging Telescope (Li et al. 2000; Filippenko et al. 2001); continued funding from the Sylvia and Jim Katzman Foundation is greatly appreciated.

Note added in proof. — P. Garnavich, A. Noriega-Crespo, & A. Moro-Martin (1996, IAU Circ., 6314) point out that SN 1994Y exhibited a strong infrared excess in data obtained about 17 months after discovery. This excess could be emission from dust formed in the ejecta, or it may be an infrared echo from an existing dust shell.

REFERENCES

- Balam, D. D. 1993, IAU Circ. 5883
- Barbon, R., Benetti, S., Cappellaro, E., Patat, F., Turatto, M., & Iijima, T. 1995, A&AS, 110, 513
- Benetti, S., Mendes de Oliveira, C., & Machado, A. 1995, IAU Circ. 6135
- Bessell, M. S. 1990, PASP, 102, 1181
- Boattini, A., & Tombelli, M. 1994, IAU Circ. 6065
- Burstein, D., & Heiles, C. 1984, ApJS, 54, 33

- Cappellaro, E., & Bragaglia, A. 1993, IAU Circ. 5888
- Clocchiatti, A., Garcia-Lopez, R., Barker, E. S., Wren, W., & Wheeler, J. C. 1994, IAU Circ. 6065
- Djorgovski, S., Thompson, D., & Smith, J. 1994, IAU Circ. 5946
- Doggett, J. B., & Branch, D. 1985, AJ, 90, 2303
- Dressler, A., & Sargent, W. 1993, IAU Circ. 5870
- Filippenko, A. V. 1992, in *Robotic Telescopes in the 1990s*, ed. A. V. Filippenko (San Francisco: ASP, Conf. Ser. Vol. 34), 55
- Filippenko, A. V. 1997, ARA&A, 35, 309
- Filippenko, A. V., & Matheson, T. 1993, IAU Circ. 5870
- Filippenko, A. V., & Matheson, T. 1994, IAU Circ. 5923
- Filippenko, A. V., Matheson, T., & Barth, A. J. 1994, IAU Circ. 6001
- Filippenko, A. V., Porter, A. C., Sargent, W. L. W., & Schneider, D. P. 1986, AJ, 92, 1341
- Filippenko, A. V., Li, W. D., Treffers, R. R., & Modjaz, M. 2001, in *IAU Conf. Ser. 246, Small-Telescope Astronomy on Global Scales*, ed. W. P. Chen, C. Lemme, & B. Paczynski (San Francisco: ASP), 121
- Hamuy, M., Phillips, M. M., Maza, M., Wischnjewsky, M., Uomoto, A., Landolt, A. U., & Khatwani, R. 1991, AJ, 102, 208
- Iijima, T., Cappellaro, E., & Turatto, M. 1994, IAU Circ. 6108
- Jiang, X. J., Liu, W., & Hu, J. Y. 1994, IAU Circ. 6065
- Kirshner, R. P. 1990, in *Supernovae*, ed. A. G. Petschek (New York: Springer-Verlag)
- Kushida, R., Nakano, S., & Kushida, Y. 1995, IAU Circ. 6134
- Landolt, A. U. 1992, AJ, 104, 340
- Leibundgut, B. 1988, Ph.D. Thesis, University of Basel
- Leibundgut, B. 1996, in *Supernovae and Supernova Remnants*, ed. R. McCray & Z. Wang (Cambridge: Cambridge University Press), 11
- Li, W. D., et al. 2000, in *Cosmic Explosions*, ed. S. S. Holt & W. W. Zhang (New York: AIP), 103
- Miller, D. L., & Branch, D. 1990, AJ, 100, 530
- Mueller, J. 1993, IAU Circ. 5870
- Mueller, J., & Mendenhall, J. D. 1994, IAU Circ. 5946
- Nakano, S., Kushida, Y., & Kushida, R. 1994, IAU Circ. 6110
- Nakano, S., Takamizawa, T., Kushida, R., & Ikeya, K. 1994, IAU Circ. 6109
- Paik, Y., Filippenko, A. V., Treffers, R. R., Van Dyk, S. D., & Richmond, M. W. 1994, IAU Circ. 6058

- Patat, F., Barbon, R., Cappellaro, E., & Turatto, M. 1994, *A&A*, 282, 731
- Patat, F., Vician, Z., & Szentasko, L. 1994, *IAU Circ.* 6111
- Pollas, C. 1993, *IAU Circ.* 5888
- Pollas, C. 1994, *IAU Circ.* 5923
- Pollas, C., & Albanese, D. 1994, *IAU Circ.* 6001
- Press, W. H., Teukolsky, S. A., Vetterling, W. T., & Flannery, B. P. 1992, *Numerical Recipes in C*, 2nd ed. (Cambridge: Cambridge University Press)
- Richmond, M. W., Treffers, R. R., & Filippenko, A. V. 1993, *PASP*, 105, 1164
- Richmond, M. W., Treffers, R. R., Filippenko, A. V., & Paik, Y. 1996, *AJ*, 112, 732
- Richmond, M. W., et al. 1995, *AJ*, 109, 2121
- Riess, A. G. 1996, Ph.D. Thesis, Harvard University
- Riess, A. G., Challis, P., & Kirshner, R. 1994, *IAU Circ.* 5948
- Riess, A. G., Press, W. H., & Kirshner, R. P. 1996, *ApJ*, 473, 88
- Riess, A. G., et al. 1999, *AJ*, 117, 707
- Sadakane, K., et al. 1996, *PASJ*, 48, 51
- Schmidt, B., Kirshner, R., & Peters, J. 1994, *IAU Circ.* 5984
- Stetson, P. B. 1987, *PASP*, 99, 191
- Suntzeff, N. B. 1996, in *Supernovae and Supernova Remnants*, ed. R. McCray & Z. Wang (Cambridge: Cambridge University Press), 41
- Treffers, R. R., Filippenko, A. V., Leibundgut, B., Paik, Y., Lee, L. F. M., & Richmond, M. W. 1993, *IAU Circ.* 5870
- Tully, R. B. 1988, *Nearby Galaxies Catalog* (Cambridge: Cambridge University Press)
- Turatto, M., Cappellaro, E., Danziger, I. J., Benetti, S., Gouiffes, C., & Della Valle, M. 1993, *MNRAS*, 262, 128
- Van Dyk, S. D., Treffers, R. R., Richmond, M. W., Filippenko, A. V., & Paik, Y. B. 1994, *IAU Circ.* 6105
- Vanmunster, T., Villi, M., & Cortini, G. 1994, *IAU Circ.* 6115
- Wang, L., Li, Z. -W., Clocchiatti, A., & Wheeler, J. C. 1995, *IAU Circ.* 6135
- Wells, L. A., et al. 1994, *AJ*, 108, 2233
- Wheeler, J. C., & Harkness, R. P. 1990, *Rep. Prog. Phys.*, 53, 1467
- Wild, P. 1994, *IAU Circ.* 5982
- Wren, W. 1994, *IAU Circ.* 6058

Fig. 1.— SN 1993Y, its host galaxy UGC 2771, and field stars in the V band, imaged on 1993 November 16. In Figures 1–10 of this paper, the SN or its position is marked with an arrow.

Fig. 2.— SN 1993Z, its host galaxy NGC 2775, and field stars in the I band, imaged on 1993 November 15.

Fig. 3.— SN 1993ae, its host galaxy UGC 1071, and field stars in the V band, imaged on 1994 January 11.

Fig. 4.— SN 1994B, its host galaxy, and field stars in the V band, imaged on 1994 February 5. The SN may not be detectable in the printed image.

Fig. 5.— Template image of SN 1994C, its host galaxy, and field stars in the I band, obtained on 1997 April 12. The SN is no longer detectable in this image.

Fig. 6.— SN 1994M, its host galaxy NGC 4493, and field stars in the V band, imaged on 1994 May 14.

Fig. 7.— SN 1994Q, its host galaxy, and field stars in the V band, imaged on 1994 July 12.

Fig. 8.— SN 1994ae, its host galaxy NGC 3370, and field stars in the I band, imaged on 1995 March 30.

Fig. 9.— SN 1995D, its host galaxy NGC 2962, and field stars in the R band, imaged on 1995 March 28.

Fig. 10.— SN 1994Y, its host galaxy NGC 5371, and field stars in the R band, imaged on 1995 March 30.

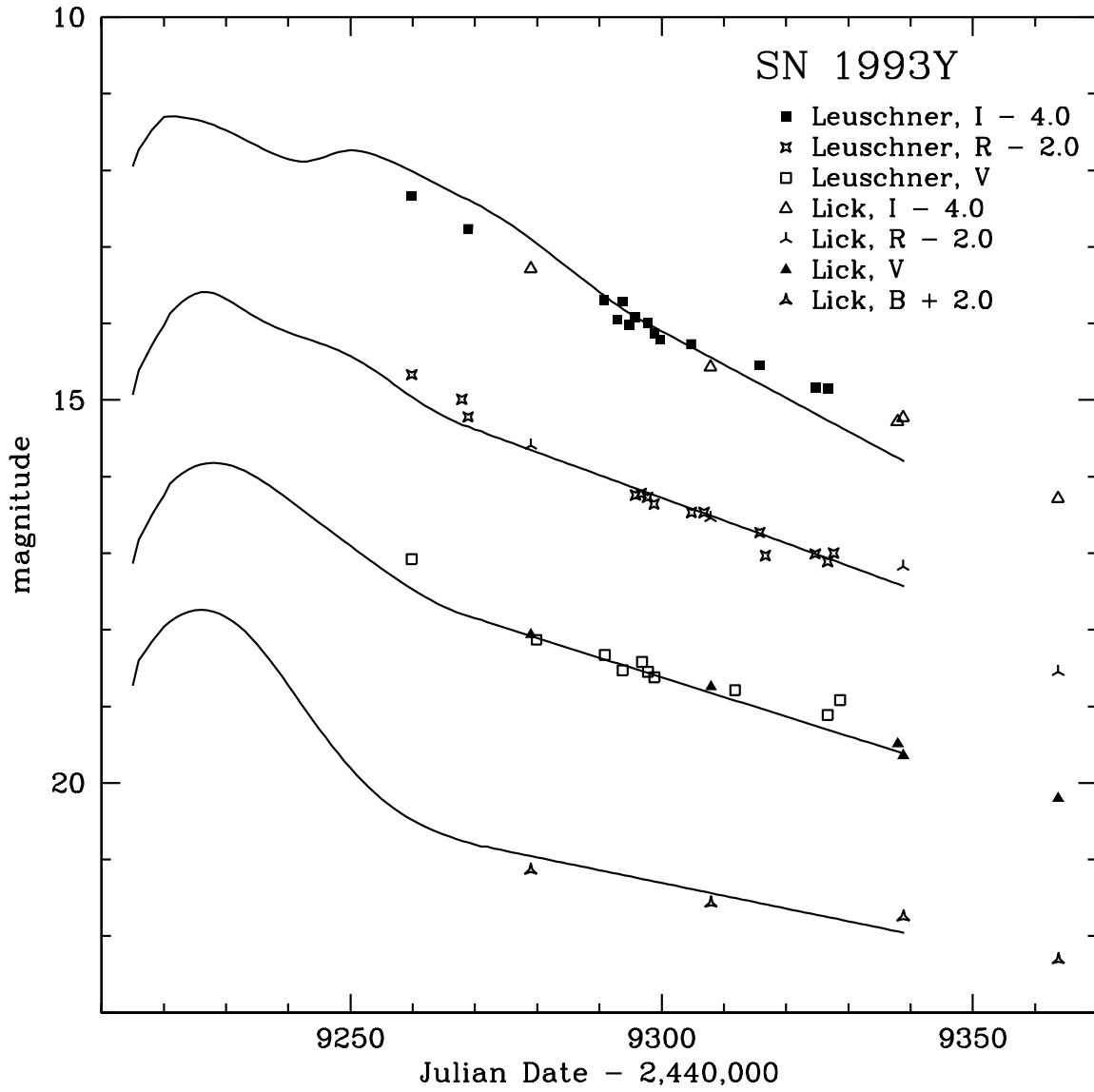


Fig. 11.— *BVRI* light curves of the Type Ia SN 1993Y. Plotted as solid lines are template Type Ia SN light curves given by Riess et al. (1996).

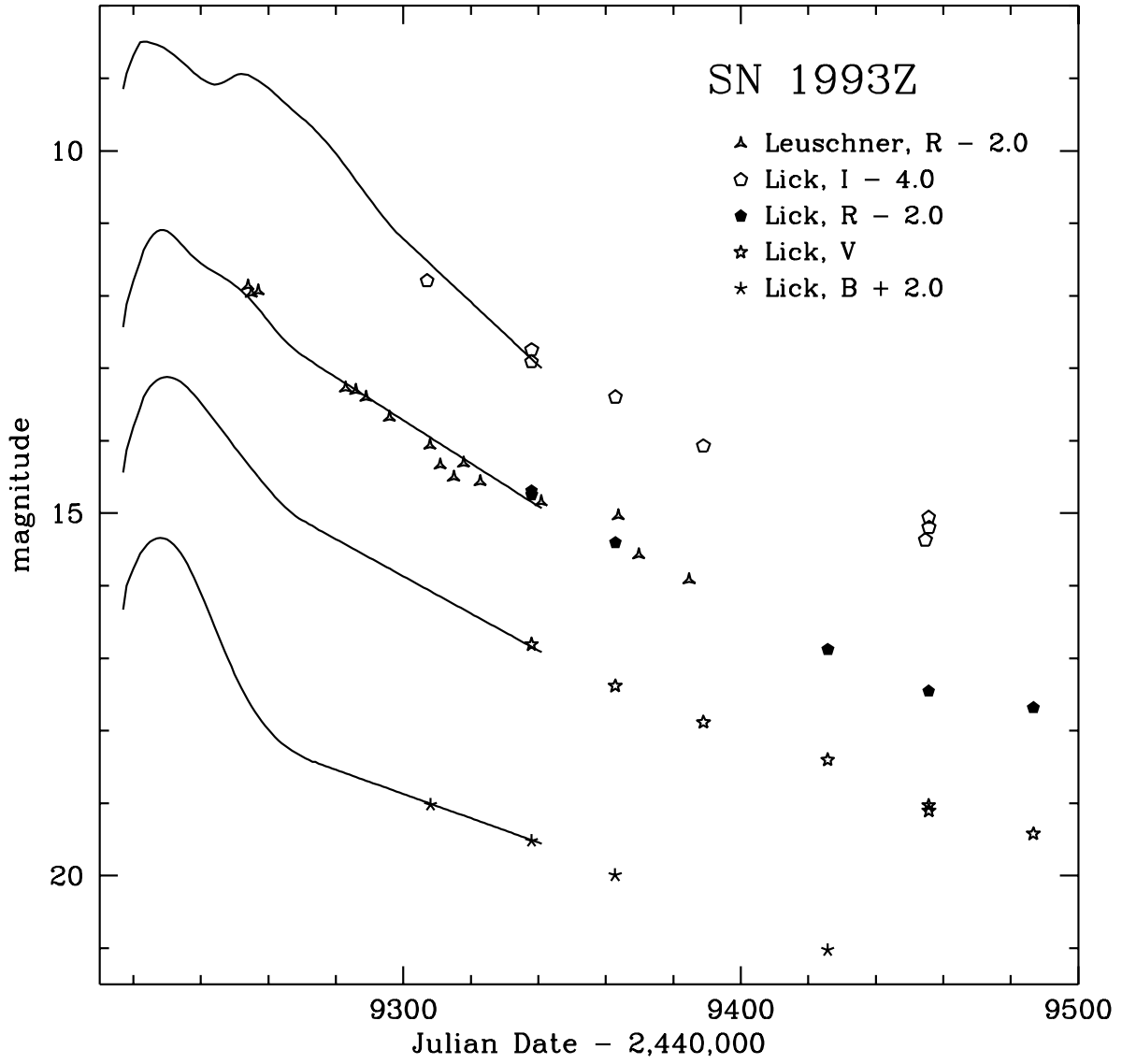


Fig. 12.— *BVRI* light curves of the Type Ia SN 1993Z. Plotted as solid lines are template Type Ia SN light curves given by Riess et al. (1996).

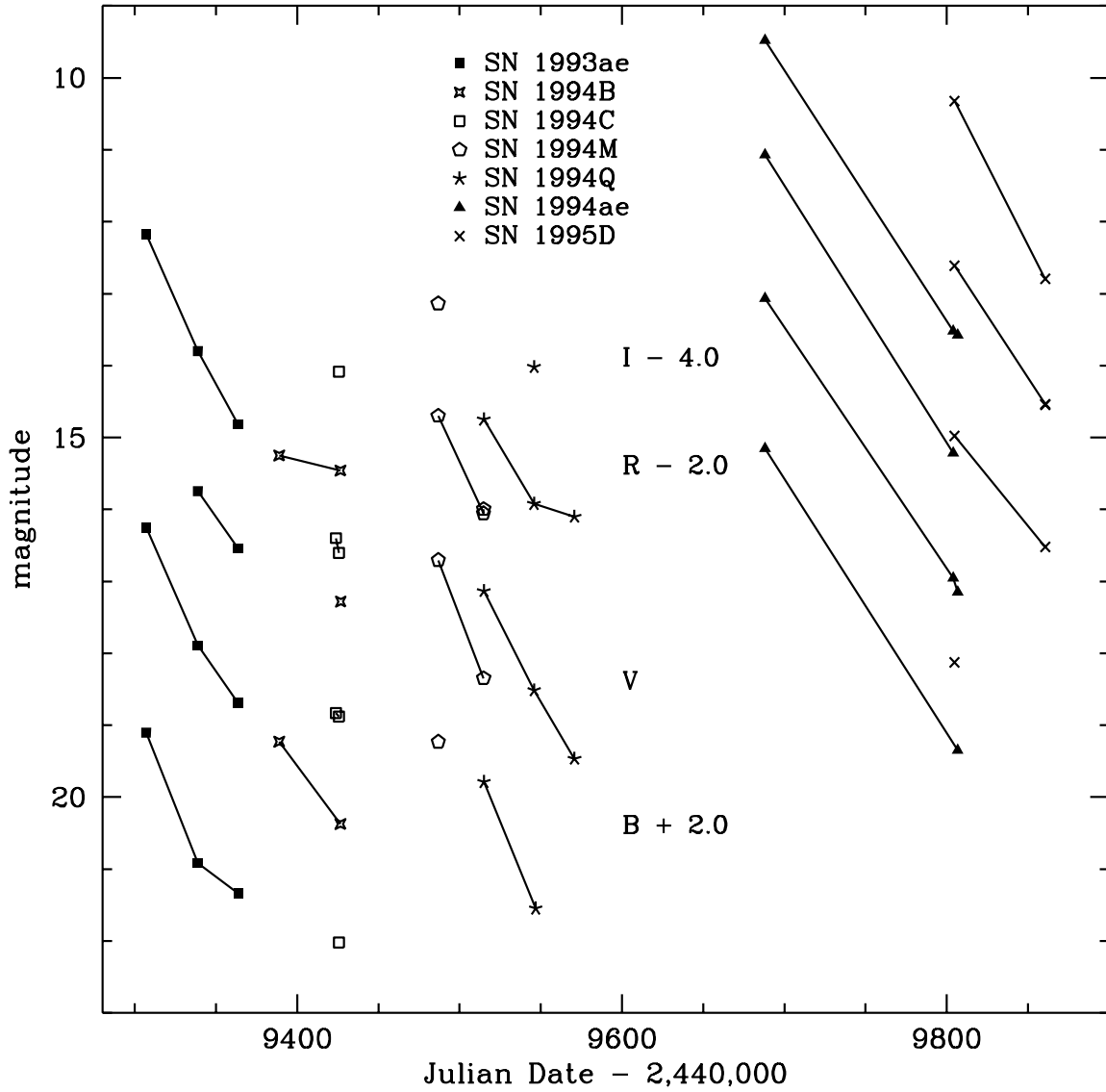


Fig. 13.— *BVRI* light curves of Type Ia supernovae. The line segments connecting the points have no significance other than to aid in distinguishing between different objects and in indicating general trends. There are no *B* measurements for SN 1994B.

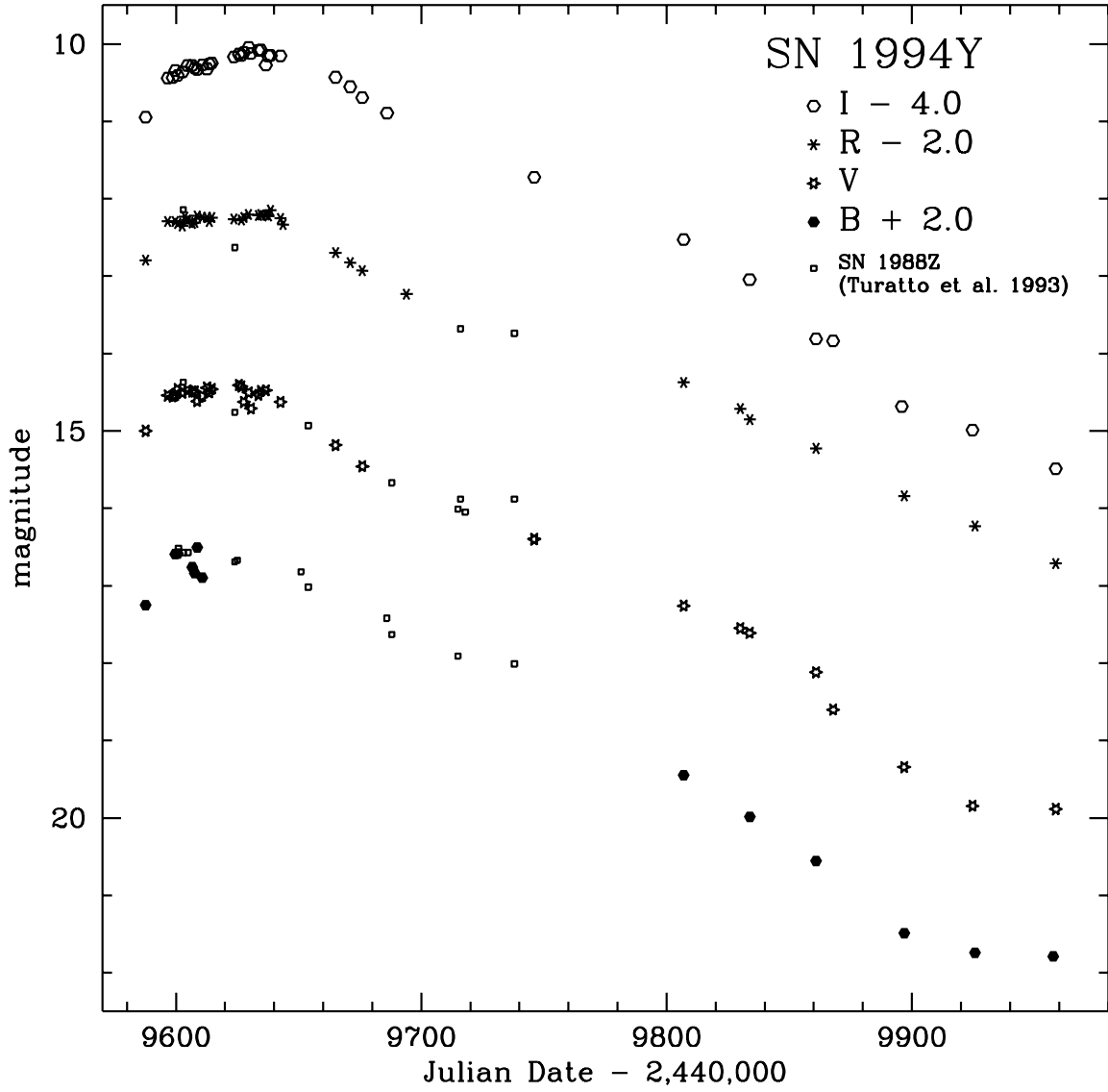


Fig. 14.— *BVRI* light curves of the Type II_n SN 1994Y. Shown for comparison are the curves for SN 1988Z.

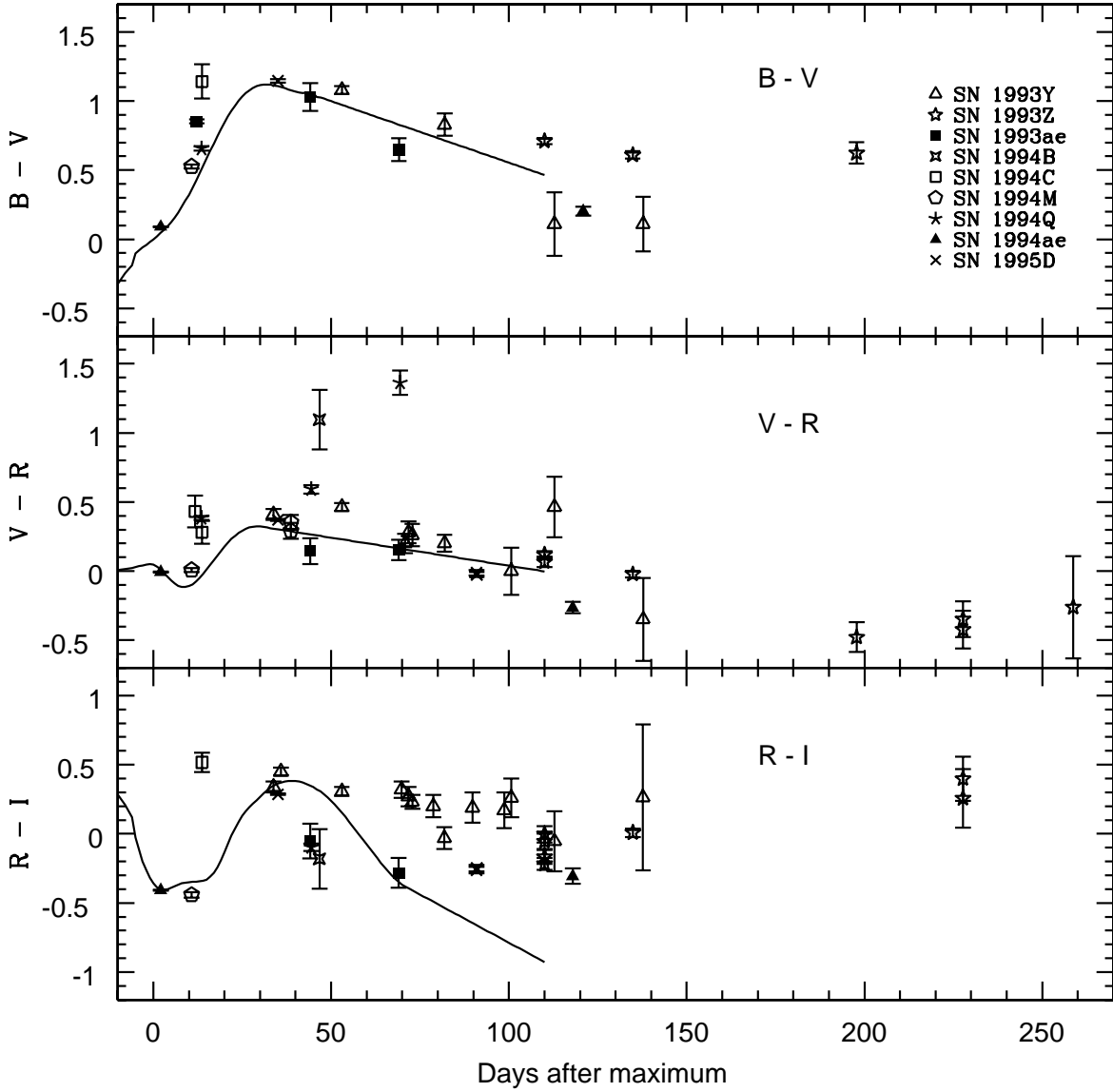


Fig. 15.— $B - V$, $V - R$, and $R - I$ color curves of Type Ia SNe. Plotted as solid lines are standard SNe Ia color curves given by Leibundgut (1988) for $B - V$ and Riess et al. (1996) for $V - R$ and $R - I$. There are large variations at late times in the $R - I$ curves given by Riess et al. (1996), so a typical curve was chosen.

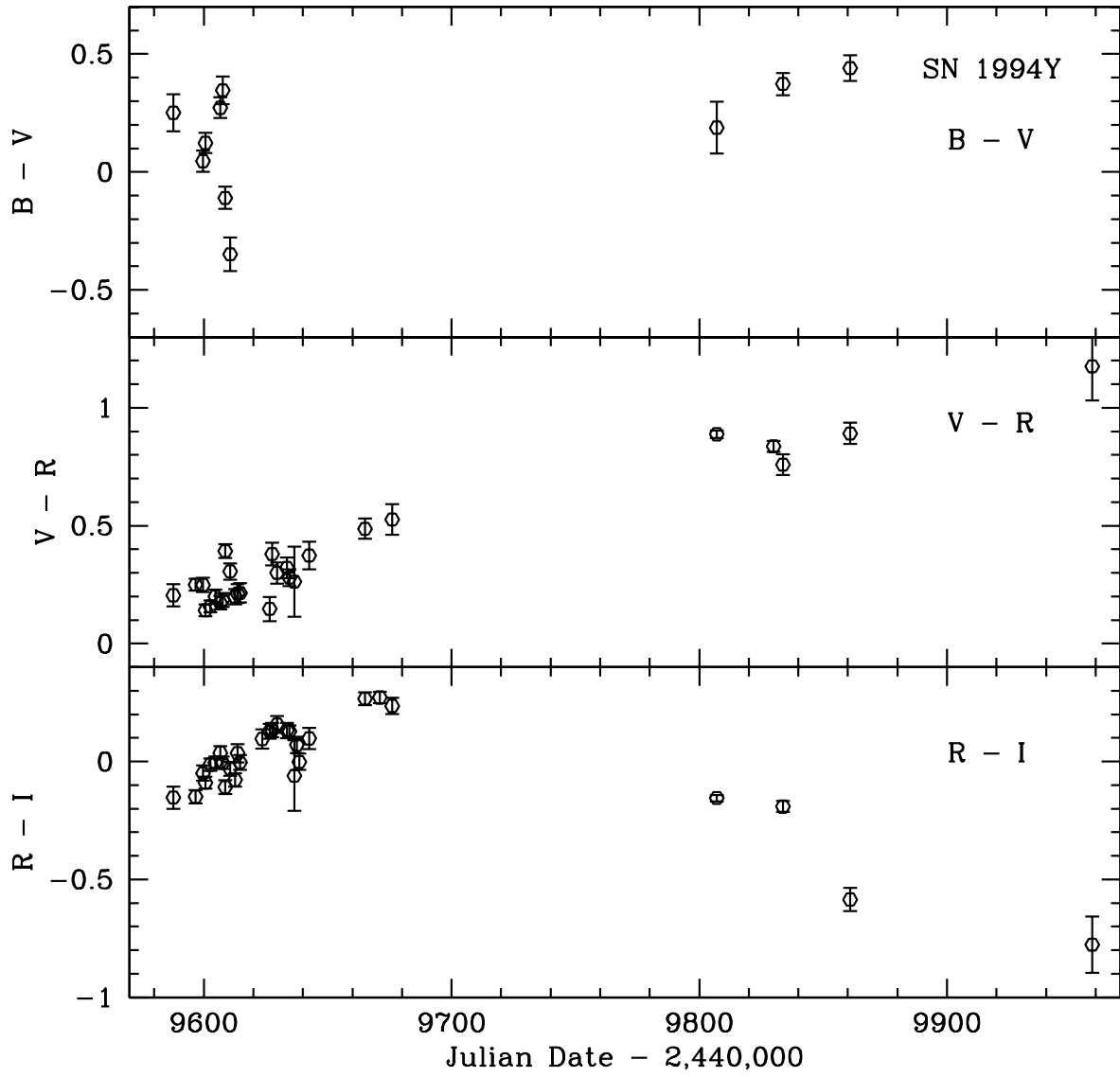


Fig. 16.— $B - V$, $V - R$, and $R - I$ color curves of the Type II_n SN 1994Y.

Table 1. Photometric solutions to transformation equations

Filter	1	coefficient		photometric night used	# of Landolt (1992) fields observed
		2	3		
SN 1993Y, 1993ae, & 1994Q					
b	4.49 (02)	0.31 (01)	−0.09 (01)	97 Sep 05	4
v	4.10 (02)	0.20 (01)	0.02 (01)		
r	3.95 (01)	0.14 (01)	0.05 (01)		
i	4.03 (03)	0.10 (01)	−0.03 (06)		
SN 1993Z & 1994ae					
b	4.09 (01)	0.28 (01)	−0.06 (00)	94 Dec 01	7
v	3.85 (01)	0.14 (01)	0.02 (01)		
r	3.74 (01)	0.11 (01)	0.04 (01)		
i	3.85 (01)	0.08 (01)	−0.02 (01)		
SN 1994C					
b	4.55 (04)	0.25 (03)	−0.07 (02)	97 Apr 12	5
v	4.04 (03)	0.25 (02)	0.02 (01)		
r	3.92 (03)	0.18 (02)	0.05 (03)		
i	4.08 (03)	0.09 (02)	−0.00 (03)		
SN 1995D					
b	4.12 (02)	0.45 (01)	−0.10 (01)	95 Mar 28	7
v	4.03 (01)	0.18 (01)	0.01 (01)		
r	3.94 (02)	0.12 (01)	0.02 (02)		
i	4.02 (02)	0.08 (01)	−0.07 (02)		
SN 1994Y					
b	4.29 (01)	0.41 (01)	−0.07 (01)	95 May 23	5
v	3.98 (02)	0.28 (01)	0.01 (01)		
r	3.86 (01)	0.24 (01)	0.01 (02)		
i	3.98 (04)	0.17 (01)	−0.04 (07)		

Table 2. Field star apparent magnitudes

star	B	V	R	I
SN 1993Y				
A	20.17 (29)	18.88 (10)	18.90 (19)	18.38 (24)
B	18.83 (10)	18.06 (05)	17.82 (08)	17.32 (10)
C	18.86 (10)	18.03 (05)	17.51 (08)	16.88 (09)
D	18.77 (10)	18.02 (05)	17.57 (08)	17.10 (09)
E	19.65 (18)	18.44 (07)	17.73 (11)	16.82 (11)
F	17.35 (03)	16.72 (01)	16.34 (02)	15.91 (03)
G	18.65 (08)	17.50 (03)	16.74 (04)	16.04 (05)
H	16.66 (02)	15.82 (01)	15.35 (01)	14.89 (01)
I	16.79 (02)	16.26 (01)	15.92 (02)	15.55 (02)
J	17.28 (02)	16.33 (01)	15.76 (02)	15.20 (02)
SN 1993Z				
A	16.04 (00)	14.87 (00)	14.15 (00)	13.49 (00)
B	16.62 (01)	15.77 (00)	15.27 (01)	14.82 (01)
C	16.65 (01)	15.79 (00)	15.31 (01)	14.86 (01)
D	18.16 (03)	17.46 (02)	17.02 (03)	16.62 (04)
E	20.45 (17)	18.97 (06)	17.93 (10)	...
F	18.94 (05)	17.83 (02)	17.11 (03)	16.57 (04)
G	17.64 (02)	17.05 (01)	16.66 (02)	16.36 (02)
SN 1993ae				
A	18.25 (08)	17.28 (03)	16.78 (04)	16.31 (05)
SN 1994B ^a				
A	15.60 (02)	14.96 (02)	14.55 (02)	14.22 (02)
B	17.11 (02)	16.53 (02)	16.16 (02)	15.84 (02)
C	16.24 (02)	15.45 (02)	14.96 (02)	14.55 (02)
D	16.12 (02)	15.58 (02)	15.23 (02)	14.94 (02)
SN 1994C				
A	18.82 (10)	18.06 (05)	17.69 (08)	17.19 (10)

Table 2—Continued

star	B	V	R	I
B	19.70 (20)	18.70 (09)	17.95 (14)	17.25 (15)
C	20.30 (29)	18.86 (10)	17.92 (16)	17.66 (17)
D	15.78 (01)	14.91 (00)	14.40 (00)	13.95 (01)
E	16.07 (01)	15.53 (00)	15.20 (01)	14.86 (01)
F	13.86 (00)	13.35 (00)	13.06 (00)	12.74 (00)
G	16.30 (01)	15.38 (00)	14.88 (01)	14.40 (01)
H	17.93 (04)	17.17 (02)	16.68 (04)	16.23 (04)
I	17.97 (04)	16.93 (02)	16.24 (03)	15.67 (03)
J	17.71 (04)	16.99 (02)	16.60 (03)	16.17 (04)
K	14.32 (00)	13.60 (00)	13.21 (00)	12.85 (00)
L	14.73 (00)	14.03 (00)	13.64 (00)	13.25 (00)
SN 1994M ^a				
A	14.20 (02)	13.19 (02)	12.68 (02)	12.32 (02)
B	15.09 (02)	14.46 (02)	14.08 (02)	13.69 (02)
SN 1994Q				
A	15.63 (01)	15.18 (00)	14.89 (01)	14.60 (01)
B	14.77 (00)	14.22 (00)	13.87 (00)	13.54 (00)
C	18.04 (04)	17.05 (02)	16.48 (03)	15.97 (03)
SN 1994ae				
A	18.07 (11)	17.58 (06)	17.13 (09)	16.58 (10)
B	19.06 (26)	18.57 (14)	17.31 (20)	15.84 (21)
C	18.84 (22)	18.34 (12)	18.02 (19)	17.93 (24)
D	18.81 (95)	20.32 (64)	18.78 (94)	18.40 (97)
E	17.18 (05)	16.53 (02)	16.11 (04)	15.66 (04)
F	18.65 (24)	18.67 (14)	18.14 (23)	17.59 (26)
G	19.06 (18)	17.66 (06)	16.52 (09)	14.95 (10)
SN 1995D				
A	18.51 (12)	17.01 (03)	16.00 (04)	14.91 (04)
B	18.22 (10)	17.21 (04)	16.61 (05)	16.15 (06)
C	14.97 (01)	14.30 (00)	13.93 (01)	13.62 (01)

Table 2—Continued

star	B	V	R	I
D	15.00 (01)	14.34 (00)	13.97 (01)	13.66 (01)
E	16.64 (03)	15.87 (01)	15.44 (02)	15.08 (02)
SN 1994Y				
A	14.27 (00)	13.93 (00)	13.74 (00)	13.62 (00)
B	14.72 (00)	14.27 (00)	13.98 (00)	13.78 (00)
C	15.81 (01)	15.35 (00)	15.08 (01)	...
D	18.57 (08)	17.66 (04)	16.83 (06)	16.24 (07)
E	18.71 (11)	18.16 (06)	17.57 (10)	17.06 (11)
F	14.77 (00)	14.19 (00)	13.82 (00)	13.53 (00)
G	18.28 (08)	17.84 (04)	17.48 (08)	17.14 (10)
H	16.54 (02)	15.92 (01)	15.54 (01)	15.27 (02)

^aUsed field star magnitudes from Riess (1996).

Table 3. SN 1993Y apparent magnitudes

UT Date	JD	B	V	R	I
SN 1993Y (Leuschner)					
93 Sep 29.34	2449259.84	...	17.08 (04)	16.67 (02)	16.33 (03)
93 Oct 07.42	2449267.92	16.99 (08)	...
93 Oct 08.41	2449268.91	17.22 (02)	16.77 (02)
93 Oct 19.40	2449279.90	...	18.13 (05)
93 Oct 30.30	2449290.80	...	18.33 (10)	...	17.70 (10)
93 Nov 01.33	2449292.83	17.95 (08)
93 Nov 02.25	2449293.75	...	18.53 (12)	...	17.71 (09)
93 Nov 03.25	2449294.75	18.01 (08)
93 Nov 04.32	2449295.82	18.24 (03)	17.92 (05)
93 Nov 05.32	2449296.82	...	18.42 (06)	18.22 (04)	...
93 Nov 06.34	2449297.84	...	18.55 (06)	18.27 (05)	18.00 (05)
93 Nov 07.33	2449298.83	...	18.62 (07)	18.36 (04)	18.13 (03)
93 Nov 08.35	2449299.85	18.21 (05)
93 Nov 13.27	2449304.77	18.47 (04)	18.27 (07)
93 Nov 15.30	2449306.80	18.47 (04)	...
93 Nov 20.31	2449311.81	...	18.79 (09)
93 Nov 24.27	2449315.77	18.73 (07)	18.54 (09)
93 Nov 25.20	2449316.70	19.03 (09)	...
93 Dec 03.17	2449324.67	19.01 (08)	18.84 (10)
93 Dec 05.17	2449326.67	...	19.11 (15)	19.11 (08)	18.85 (11)
93 Dec 06.17	2449327.67	19.00 (07)	...
93 Dec 07.17	2449328.67	...	18.92 (17)
SN 1993Y (Lick)					
93 Oct 18.50	2449279.00	19.14 (02)	18.06 (02)	17.60 (02)	17.29 (03)
93 Nov 16.40	2449307.90	19.57 (07)	18.74 (05)	18.54 (04)	18.57 (07)
93 Dec 16.43	2449337.93	...	19.49 (21)	...	19.28 (22)
93 Dec 17.34	2449338.84	19.75 (14)	19.64 (18)	19.18 (12)	19.23 (18)
94 Jan 11.24	2449363.74	20.31 (11)	20.20 (16)	20.55 (25)	20.29 (47)

Table 4. SN 1993Z apparent magnitudes

UT Date	JD	B	V	R	I
SN 1993Z (Leuschner)					
93 Sep 23.52	2449254.02	13.87 (07)	...
93 Sep 24.52	2449255.02	13.96 (08)	...
93 Sep 26.53	2449257.03	13.94 (08)	...
93 Oct 22.45	2449282.95	15.27 (17)	...
93 Oct 25.44	2449285.94	15.31 (17)	...
93 Oct 28.45	2449288.95	15.40 (18)	...
93 Nov 04.42	2449295.92	15.68 (20)	...
93 Nov 16.39	2449307.89	16.06 (24)	...
93 Nov 19.48	2449310.98	16.34 (26)	...
93 Nov 23.46	2449314.96	16.50 (28)	...
93 Nov 26.38	2449317.88	16.31 (26)	...
93 Dec 01.36	2449322.86	16.57 (28)	...
93 Dec 19.37	2449340.87	16.84 (31)	...
93 Jan 11.28	2449363.78	17.03 (33)	...
93 Jan 17.29	2449369.79	17.57 (38)	...
93 Feb 01.27	2449384.77	17.92 (42)	...
SN 1993Z (Lick)					
93 Nov 15.57	2449307.07	15.79 (01)
93 Nov 16.57	2449308.07	17.02 (02)
93 Dec 16.52	2449338.02	17.52 (02)	16.81 (01)	16.69 (02)	16.91 (04)
				16.74 (03)	16.75 (05)
94 Jan 10.32	2449362.82	17.99 (02)	17.38 (02)	17.40 (02)	17.40 (02)
94 Feb 05.43	2449388.93	...	17.88 (03)	...	18.07 (05)
94 Mar 14.29	2449425.79	19.02 (06)	18.40 (05)	18.88 (10)	...
94 Apr 12.21	2449454.71	19.37 (42)
94 Apr 13.22	2449455.72	...	19.03 (09)	19.45 (10)	19.06 (12)
			19.11 (08)		19.20 (19)
94 May 14.22	2449486.72	...	19.42 (16)	19.68 (34)	...

Table 5. SN Ia apparent magnitudes (Lick)

UT Date	JD	B	V	R	I
SN 1993ae					
93 Nov 15.34	2449306.84	17.10 (01)	16.25 (01)	...	16.17 (01)
93 Dec 17.21	2449338.71	18.92 (09)	17.89 (05)	17.75 (08)	17.80 (10)
94 Jan 11.14	2449363.64	19.34 (06)	18.69 (05)	18.54 (05)	18.82 (10)
SN 1994B					
94 Feb 05.37	2449388.87	...	19.23 (04)	...	19.25 (07)
94 Mar 15.23	2449426.73	...	20.38 (17)	19.28 (13)	19.46 (17)
SN 1994C					
94 Mar 12.27	2449423.77	...	18.83 (07)	18.40 (09)	...
94 Mar 14.20	2449425.70	20.02 (11)	18.88 (06)	18.60 (06)	18.08 (04)
SN 1994M					
94 May 14.33	2449486.83	17.23 (01)	16.71 (01)	16.70 (01)	17.14 (02)
94 Jun 11.27	2449514.77	...	18.35 (04)	18.06 (04)	...
				18.00 (04)	
SN 1994Q					
94 Jun 11.43	2449514.93	17.79 (01)	17.13 (01)	16.75 (01)	...
94 Jul 12.35	2449545.85	...	18.51 (02)	17.92 (02)	18.02 (02)
94 Jul 13.40	2449546.90	19.55 (07)
94 Aug 06.28	2449570.78	...	19.46 (07)	18.10 (05)	...
SN 1994ae					
94 Dec 01.58	2449688.08	13.15 (00)	13.06 (00)	13.07 (00)	13.48 (00)
95 Mar 27.44	2449803.94	...	16.95 (02)	17.22 (03)	17.52 (04)
95 Mar 30.36	2449806.86	17.35 (02)	17.15 (03)	...	17.58 (03)

Table 5—Continued

UT Date	JD	B	V	R	I
SN 1995D					
95 Mar 28.33	2449804.83	16.12 (01)	14.98 (00)	14.61 (00)	14.32 (00)
95 May 23.23	2449860.73	...	16.52 (01)	16.53 (02)	16.80 (02)
				16.55 (01)	

Table 6. SN 1994Y apparent magnitudes

UT Date	JD	B	V	R	I
SN 1994Y (Leuschner)					
94 Aug 22.17	2449587.67	15.25 (07)	15.00 (04)	14.79 (03)	14.95 (04)
94 Aug 31.16	2449596.66	...	14.54 (02)	14.29 (02)	14.44 (02)
94 Sep 09.16	2449598.66	...	14.55 (02)	...	14.44 (03)
94 Sep 03.16	2449599.66	14.59 (04)	14.54 (02)	14.30 (02)	14.34 (03)
94 Sep 04.19	2449600.69	14.58 (04)	14.46 (02)	14.32 (01)	14.41 (02)
94 Sep 06.15	2449602.65	...	14.51 (02)	14.35 (02)	14.36 (02)
94 Sep 07.15	2449603.65	14.23 (02)	...
94 Sep 08.20	2449604.70	...	14.48 (02)	14.28 (01)	14.28 (02)
94 Sep 10.15	2449606.65	14.76 (04)	14.49 (02)	14.32 (02)	14.28 (02)
94 Sep 11.19	2449607.69	14.84 (05)	14.49 (03)	14.31 (01)	14.31 (02)
94 Sep 12.15	2449608.65	14.50 (04)	14.62 (02)	14.22 (02)	14.33 (02)
94 Sep 14.19	2449610.69	14.90 (06)	14.55 (03)	14.24 (02)	14.27 (02)
94 Sep 16.18	2449612.68	...	14.44 (03)	14.24 (02)	14.32 (02)
94 Sep 17.14	2449613.64	...	14.50 (03)	14.29 (02)	14.26 (03)
94 Sep 18.18	2449614.68	...	14.46 (04)	14.24 (02)	14.25 (02)
94 Sep 27.13	2449623.63	14.26 (03)	14.17 (03)
94 Sep 29.13	2449625.63	...	14.41 (03)	...	14.13 (02)
94 Sep 30.13	2449626.63	...	14.42 (05)	14.28 (02)	14.15 (02)
94 Oct 01.13	2449627.63	...	14.62 (04)	14.24 (02)	14.11 (02)
94 Oct 03.12	2449629.62	...	14.50 (04)	14.20 (02)	14.05 (03)
94 Oct 04.12	2449630.62	...	14.71 (07)	...	14.12 (04)
94 Oct 07.12	2449633.62	...	14.53 (04)	14.21 (02)	14.08 (02)
94 Oct 08.12	2449634.62	...	14.49 (03)	14.21 (02)	14.08 (02)
94 Oct 10.12	2449636.62	...	14.48 (13)	14.21 (07)	14.27 (14)
94 Oct 11.11	2449637.61	14.22 (02)	14.15 (03)
94 Oct 12.11	2449638.61	14.15 (02)	14.15 (03)
94 Oct 16.11	2449642.61	...	14.63 (05)	14.25 (03)	14.15 (03)
94 Oct 17.10	2449643.60	14.33 (03)	...
94 Nov 08.54	2449665.04	...	15.18 (04)	14.70 (02)	14.43 (02)
94 Nov 14.55	2449671.05	14.82 (02)	14.55 (02)
94 Nov 19.51	2449676.01	...	15.46 (06)	14.93 (02)	14.69 (02)
94 Nov 29.56	2449686.06	14.89 (02)
94 Dec 07.51	2449694.01	15.23 (03)	...

Table 6—Continued

UT Date	JD	B	V	R	I
SN 1994Y (KPNO)					
95 Jan 28.51	2449746.01	...	16.40 (03) 16.40 (05)	...	15.72 (02)
SN 1994Y (Lick)					
95 Mar 30.53	2449807.03	17.45 (11)	17.26 (01)	16.37 (01)	16.53 (01)
95 Apr 22.51	2449830.01	...	17.55 (02)	16.71 (02)	...
95 Apr 26.37	2449833.87	17.98 (02)	17.61 (04)	16.85 (02)	17.04 (01)
95 May 23.45	2449860.95	18.56 (07)	18.12 (03)	17.23 (04)	17.81 (04)
95 May 30.40	2449867.90	...	18.60 (04)	...	17.84 (02)
95 Jun 27.34	2449896.84	...	19.34 (08)	...	18.68 (05)
95 Jun 28.36	2449897.86	19.49 (13)	...	17.84 (03)	...
95 Jul 25.27	2449924.77	...	19.84 (10)	...	18.99 (07)
95 Jul 26.28	2449925.78	19.74 (10)	...	18.23 (05)	...
95 Aug 27.15	2449957.65	19.79 (23)
95 Aug 28.17	2449958.67	...	19.89 (13)	18.71 (06)	19.49 (10)

Table 7. Supernova late-time decline rates, mag/100 days

	γ_B	γ_V	γ_R	γ_I	reference
Type Ia SNe					
SN 1993Y	1.33 ± 0.11	2.62 ± 0.10	2.94 ± 0.08	3.89 ± 0.11	
SN 1993Z	1.74 ± 0.04	1.94 ± 0.03	2.49 ± 0.05	2.72 ± 0.04	
SN 1980N	1.6 ± 0.3	2.1 ± 0.3	Hamuy et al. 1991
SN 1989B	1.4 ± 0.1	2.4 ± 0.2	Wells et al. 1994
Type II SNe					
SN 1994Y	...	1.44 ± 0.03	1.59 ± 0.02	...	
SN 1988Z	0.47	0.44	0.18	...	Turatto et al. 1993
SN 1993J	1.22 ± 0.08	1.41 ± 0.07	1.24 ± 0.04	1.48 ± 0.06	Richmond et al. 1996

Table 8. SN 1994Y peak magnitudes

	B	V	R	I
JD	2449603.7 ± 0.5	2449617.7 ± 3.0	2449618.5 ± 4.0	2449629.0 ± 2.0
UT	Sep 07.20	Sep 21.20	Sep 22.00	Oct 03.50
m_{max}	14.52 ± 0.04	14.36 ± 0.05	14.14 ± 0.02	14.04 ± 0.04
M_{max}	-18.37	-18.53	-18.75	-18.85

This figure "f1.jpg" is available in "jpg" format from:

<http://arxiv.org/ps/astro-ph/0108299v2>

This figure "f2.jpg" is available in "jpg" format from:

<http://arxiv.org/ps/astro-ph/0108299v2>

This figure "f3.jpg" is available in "jpg" format from:

<http://arxiv.org/ps/astro-ph/0108299v2>

This figure "f4.jpg" is available in "jpg" format from:

<http://arxiv.org/ps/astro-ph/0108299v2>

This figure "f5.jpg" is available in "jpg" format from:

<http://arxiv.org/ps/astro-ph/0108299v2>

This figure "f6.jpg" is available in "jpg" format from:

<http://arxiv.org/ps/astro-ph/0108299v2>

This figure "f7.jpg" is available in "jpg" format from:

<http://arxiv.org/ps/astro-ph/0108299v2>

This figure "f8.jpg" is available in "jpg" format from:

<http://arxiv.org/ps/astro-ph/0108299v2>

This figure "f9.jpg" is available in "jpg" format from:

<http://arxiv.org/ps/astro-ph/0108299v2>

This figure "f10.jpg" is available in "jpg" format from:

<http://arxiv.org/ps/astro-ph/0108299v2>